Sixth International Symposium on Marine Propulsors
smp'19, Rome, Italy, May 2019

The Effect of Rudder Existence on the Propeller Eccentric Forces

Gi-Su Song[1], Tae-Goo Lee[1], and Hyoung-Gil Park[1]

[1]SSMB(Samsung Ship Model Basin), Marine Research Institute, Samsung Heavy Industries Co., Ltd., Dae-jeon, Republic of Korea

ABSTRACT

The precise prediction of the load on a stern tube bearing is essential for design of the safe shafting system in a ship. It is well known that the load on stern tube bearing is directly influenced by the eccentric forces of propeller. In this paper, the effect of rudder existence on propeller eccentric forces has been studied based on numerical analysis for 10K Class container vessel. To obtain the propeller eccentric forces, the numerical simulations including propeller rotation motion using the sliding mesh technique were carried out. When the ship is turning, the propeller eccentric forces are significantly changed comparing to those of straight run. For STBD turning of ship, especially, the propeller vertical moment would be decreased about 50% due to the rudder existence comparing to that in case without rudder. In contrast, it is similar each other regardless of rudder existence for PORT turning. This difference is fundamentally oriented by the interaction between propeller's rotation and inflow to propeller. Based on this study, it is inferred that the influence of appendages around propeller would be considered for reliable prediction of propeller eccentric forces.

Keywords

Propeller Eccentric forces, Rudder, Shaft forces, Turning, Manoeuvring

1 INTRODUCTION

The safe design of shafting system on a ship has been important issue for a long time. If unexpected problem on the shafting system occurs in voyage with harsh sea condition, this is directly connected to the safety of people on the ship. Therefore the shafting system has been designed conservatively by strict guidance of classification. In general, the shafting system contains propeller, shaft, bearings and so on. Especially, the load on a stern tube bearing located in front of propeller is directly related to the eccentric force of propeller. Since the propeller rotates in a non-uniform wake field, eccentric forces on propeller are continuously provided, additionally, they are changed dramatically during the ship turning. Although there are many processes to be calculated or checked for the design of shafting system, unintended problem such as stern tube bearing damage has been rarely but still reported. Moreover the classifications such as ABS (2018) or DNV-GL (2018) have been announced the revised guideline for safe design of shafting system. Predicted eccentric forces of propeller from numerical simulations are used for calculating the stern tube bearing load, eventually the safety of shafting system would be secured. For this purpose, detail condition for example, draft and ship speed for reliable numerical simulations was strictly clarified at a guideline of most classifications. Besides, some researches have been conducted to design or investigate a safe shafting system for a long time according to academic interests or engineering needs. Kuriowa et al. (2007) proposed the quasi-steady method to estimate the propeller shaft forces during turning with the wakefield calculated by CFD based on the manoeuvring simulation. Vartdal et al. (2009) calculated the full scale propeller's eccentric forces using commercial RANS solver with MRF (Moving Reference Frame) method. Shin (2015) studied the effect of propeller forces on the propeller shaft bearing during straight run and turning. He simulated the nominal wake using commercial RANS solver and evaluated the eccentric forces of propeller using potential code, MPUF3A. Lee et al. (2017) investigated propeller eccentric forces and load of stern tube bearing on contra rotating propeller system, compared to those of conventional single propeller. From many previous studies, it can be inferred that there are several factors to influence on propeller eccentric forces. Among of them, we focused on the rudder's effect in this study. To analyze the effect of rudder existence, numerical simulations contained a rudder or not were conducted at same conditions for straight run or turning motion and compared each other.

2 NUMERICAL DETAIL

In this study, the target vessel was defined as about 10,000TEU class container ship. The main particulars of the ship and propeller are briefly summarized in Table. 1 and Figure 1 shows the target vessel.

Table 1. Main particulars of target vessel and propeller

LBP x B x Td	286.0m x 48.2m x 12.5m
Target speed	23 kts
Propeller Dia.	9.4m
Number of Blade	5

Figure 1 The target vessel

2.1 Validation For Numerical Simulation

Since this study was mainly carried out using the numerical approach, the reliability of our simulation was verified at first. The measured data from resistance test and POW (Propeller Open Water) test in model scale were compared to those from numerical simulation. The computational domain and boundary condition are represented in Figure 2 and Figure 3, respectively. The fundamental information for numerical simulation is shown in Table 2.

Table 2. Numerical method

Code	STAR-CCM+ Ver. 10.06
Governing Equation	RANS
Turbulence model	Reynolds Stress Model
Convection term	2nd Upwind scheme
Grid system	Trimmer :around Ship Polyhedral : around propeller
Computation Domain for Resistance test	Longitudinal length : 5.0L Transverse length : 5.0L Vertical length : 1.8L
Computation Domain for POW test	Outer Diameter : 4.0D Longitudinal length : 8.0D
Number of Grids for Resistance test	About 3.2M
Number of Grids for POW test	About 2.2M

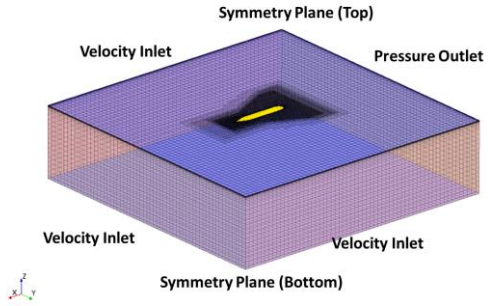

Figure 2 Computational domain and boundary condition for resistance test

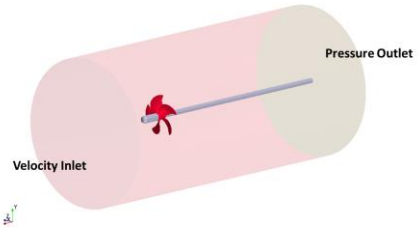

Figure 3 Computational domain and boundary condition for POW simulation

The numerical simulation for resistance test was carried out at several ship speeds (from 19kts to 25kts). The free surface for realistic wave elevation around ship was described by using VOF method. As shown in Figure 4, the difference of EHP between model test and numerical simulation was less than 2% at design draft in all Froude number. And the result of POW simulation is presented in Figure 5. The advance ratio, J, is determined from 0.5 to 0.8 with interval, 0.05 for numerical simulation. The difference of thrust coefficient (K_T) and the torque coefficient (K_Q) between CFD simulation and model test is less than 2%. And the efficiency(η_o) evaluated by CFD simulation is very similar to the those from model test. Based on these results we judged that our numerical simulations have the reliability for this study.

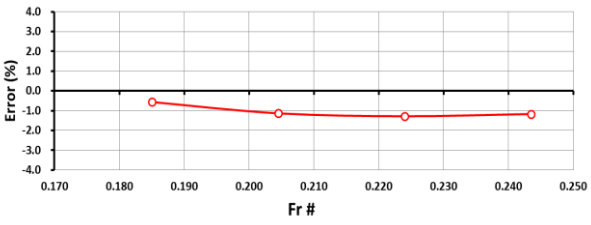

Figure 4 Difference between model test and CFD simulation at various ship speed in resistance test

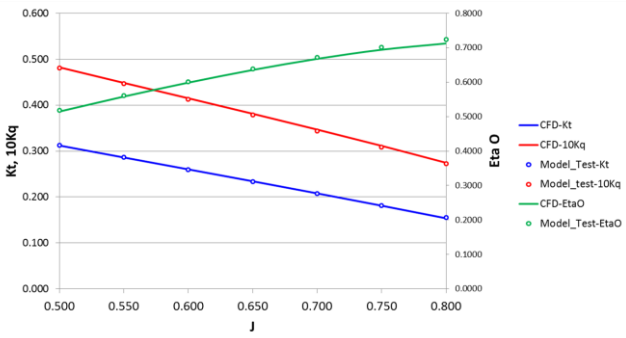

Figure 5 Comparison of thrust & torque coefficient and efficiency from model test and CFD simulation at various advance ratio (J)

2.2 Definition For Manoeuvring Condition

As mentioned, the propeller during ship turning experiences the continuous inflow changing. To simply describe this circumstance, we applied the quasi-steady approach suggested by Kuoiwa et al. (2007). It is a method to define the flow angle against the propeller plane at a specific instant during ship turning by calculating the actual drift angle. The actual drift angle is calculated by equation (1). The definition of variables in equation (1) is schematically presented in Figure 6.

$$\alpha = \beta + tan^{-1}\left(\frac{x_p}{U}\cdot r\right) \approx \beta + \frac{x_p}{U}\cdot r \qquad (1)$$

where x_p = Distance from the propeller to the gravitational center of the hull; U = Velocity of the ship; and β = Drifting angle

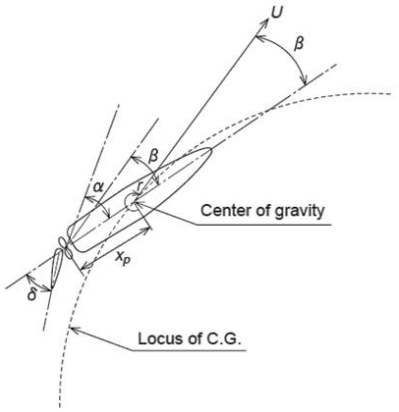

Figure 6 Inflow angle into propeller during ship turning (Kuoiwa et al. (2007))

Figure 7 and Figure 8 represent the measured values such as yaw rate, and propeller rpm of full-scale ship during turning circle test in official sea trial, respectively. From these Figures, we could recognize that the ship in turning motion reaches to the point of maximum yaw rate status, called "Yaw Rate Max", in a short time just after the turning test starts. About 300sec later, the yaw rate is converged and ship speed also become stable, and this status is called as "Steady". It is known that the inflow conditions to propeller of these two situations are quite different to that of straight run, so eccentric forces induced by propeller may be also different. Table 3 represents the inflow conditions. The numerical simulations for prediction of propeller eccentric forces in these conditions were carried out based on validated methodologies referred in previous section 2.1. The approach ship speed and propeller's rotation speed were determined by referring the sea trial data in Figure 7 and Figure 8. Although the wave is naturally generated in straight run and turning of ship, free surface does not affect directly to flow into propeller. So, the free surface was not considered and replaced as the symmetry boundary condition. And this approach has advantages such as the reduction of computing time, cost and numerical instability of CFD simulation. The rotation of propeller was realized by implementation of sliding technique and propeller eccentric forces could be directly calculated on simulation.

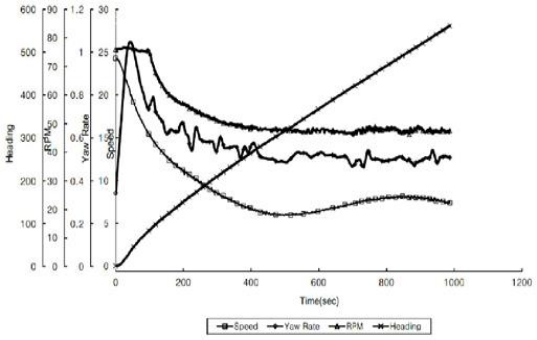

Figure 7 Ship motion during turning circle test (STBD turning) in the sea trial

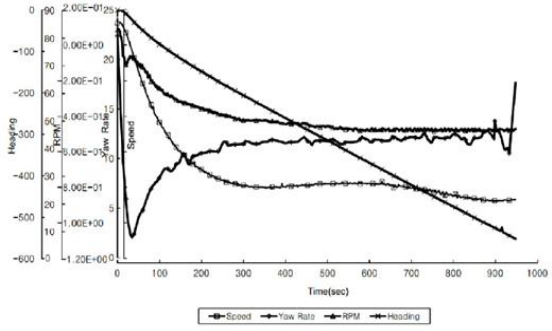

Figure 8 Ship motion during turning circle test (PORT turning) in the sea trial

Table 3. Information of the turning rate at three representative inflow conditions

Turning Status	Turning Direction	Yaw Rate (deg./sec.)	Actual Drift Angle (deg.)
Straight Run	-	0	0
Yaw Rate Max	PORT Turn	-1.01	22.45
	STBD Turn	0.99	-22.15
Steady	PORT Turn	-0.80	27.04
	STBD Turn	0.79	-26.20

2.3 Rudder Configuration

The schematic of asymmetric spade rudder installed on target vessel is presented in Figure 9. The section shape which is different at rudder's upper part & lower part was applied for preventing rudder cavitation. And energy saving device such as rudder bulb or post-swirl stator was not considered.

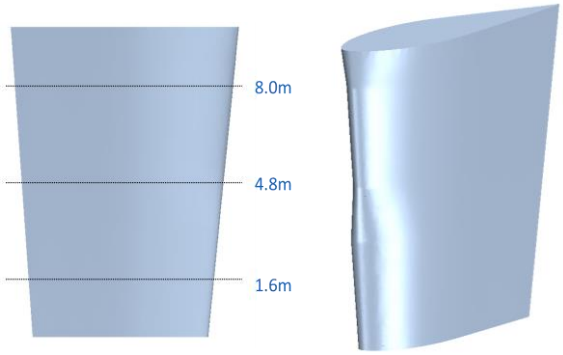

Figure 9 Asymmetric rudder configurations

2.4 Coordinate System

The coordinate system for analysis of propeller eccentric forces was defined as shown in Figure 10.

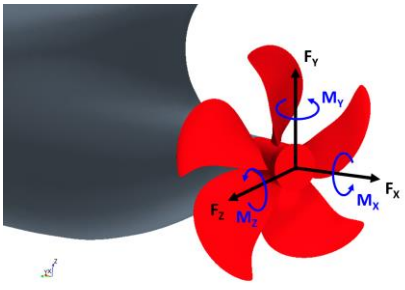

Figure 10 The coordinate system for propeller lateral forces and moments

3 RESULT

To investigate the rudder effect on propeller eccentric forces, simulation cases were categorized as two parts: straight run and turning conditions including STBD and PORT direction. And propeller lateral forces and moments were evaluated by averaging for last 1 revolution of propeller. The propeller's rotation angle per each time step is defined as 1° for realistic simulation.

3.1 Straight Run

The nominal wake distributions evaluated by numerical simulation and measured by model test on straight run were compared in Figure 11, respectively. In model test, the rudder does not exist due to the measuring equipment composed by pitot tube and traverse system. To compare the rudder effect, two numerical simulations were carried out with rudder or without.

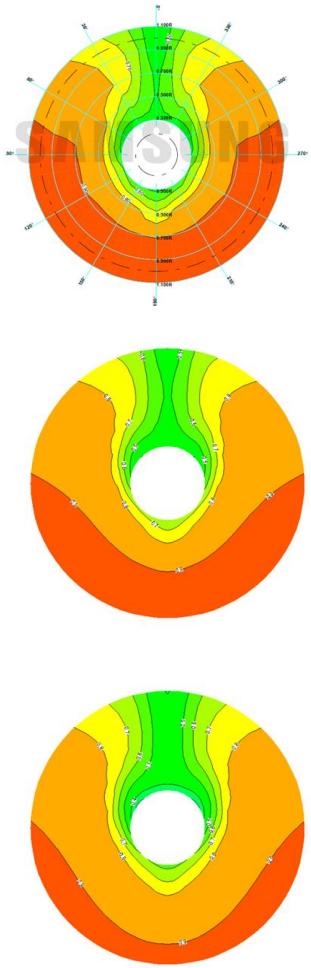

Figure 11 Nominal wake distribution

(Top: Model test, Mid.:Simulation without rudder,

Bottom: Simulation with rudder)

As known from Figure 11, the wake distribution in upper part of propeller (from 9 o'clock to 3 o'clock) from numerical simulation without rudder and model test is quite similar to each other. If the rudder exists, the axial velocity is decelerated on vertical center-line. In Table 4, the thrust and torque of propeller with rudder and without rudder was presented, respectively.

Table 4. Change of thrust and torque by rudder existence on straight run

	w/ Rudder	w/o Rudder
Thrust (Fx)	112%	100%
Torque (Mx)	107%	100%

Thrust and torque of propeller with rudder are larger than those of propeller without rudder. Due to the rudder, the inflow velocity to propeller is reduced, consequently the angle of attack of propeller is relatively larger. Since the increment of thrust is bigger than that of torque with rudder, the propulsive efficiency of propeller would be increased. Figure 12 shows the instantaneous pressure distribution on propeller face side, the difference is shown. Moreover, pressure on the propeller cap-end surface also increased. This is well known phenomenon as "wake effect".

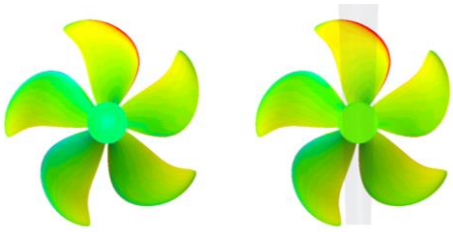

Figure 12 Instantaneous pressure distribution on propeller face side (looking upstream) during straight run

(Left: without rudder, Right: with rudder)

3.2 Turning Condition

The ratio of propeller lateral forces and moments in turning condition for the thrust and torque in straight run is presented from Figure 13 to Figure 16, including rudder or not. During STBD turning with rudder, the change of the vertical moment (Mz) directly related to the load of stern tube bearing is remarkable comparing to those values without rudder. By existence of rudder, the vertical moment (Mz) is reduced about 50% and this is effective for alleviation of load on a stern tube bearing. This tendency was similar regardless turning status (Yaw Rate Max or Steady). On the other hands, the vertical moment (Mz) with rudder is almost similar to that value without rudder during PORT turning. From above results, it is summarized that the effect of rudder existence on the vertical moment (Mz) is asymmetric as the turning direction. The reason is essentially oriented by the interaction between propeller's rotation direction and inflow direction. During STBD turning motion, the direction of flow into propeller is from PORT side to STBD side. Since the propeller rotate clockwise, it continuously experiences a count-swirl flow in lower part on the propeller(from 9 o'clock to 3 o'clock) during ship turning motion. Figure 17 presents the instantaneous pressure distribution on face side of propeller without rudder in both turning status, and it is known that the thrust center of propeller naturally locates in lower part on the propeller.

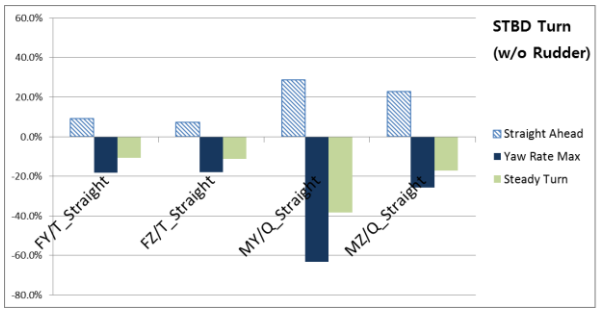

Figure 13 Propeller lateral force and moment during STBD turn (without Rudder)

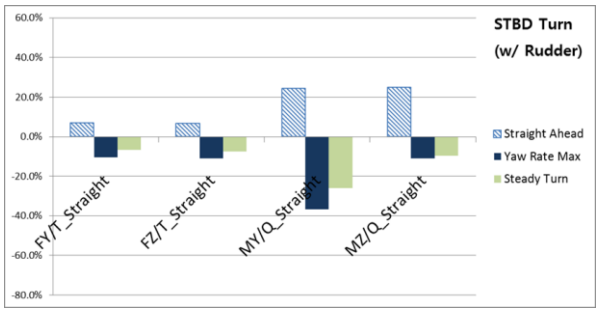

Figure 14 Propeller lateral force and moment during STBD turn (with Rudder)

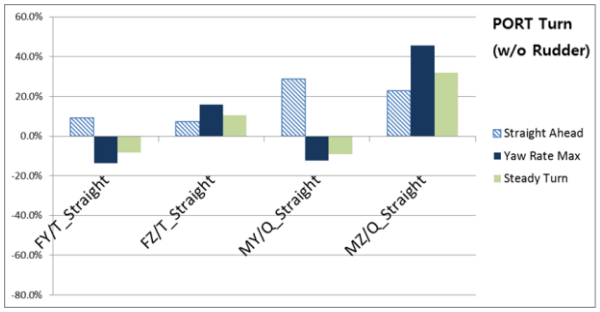

Figure 15 Propeller lateral force and moment during PORT turn (without Rudder)

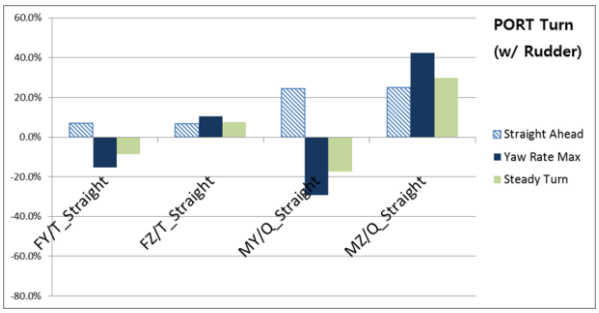

Figure 16 Propeller lateral force and moment during PORT turn (with Rudder)

If the rudder exists, in contrast, the pressure on upper part of propeller is much increased, as shown in Figure 18. Of course, the pressure on lower part of propeller was somewhat increased but the effect was restricted. Because

the upper region of rudder is relatively closer to propeller than the lower region of rudder by sweep angle. And this tendency is similar regardless turning status, namely, yaw rate max or steady. And Figure 19 shows the instantaneous pressure distribution on plane defined at several height above baseline in yaw rate max status. Especially, the difference of results simulated with rudder or not is clearly contrasted at upper region of rudder.

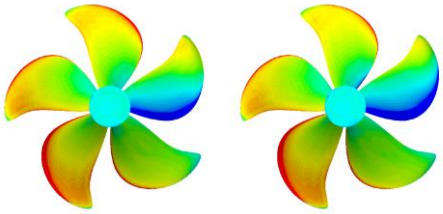

Figure 17 Instantaneous pressure distribution on propeller face side without rudder during STBD turning

(Left: at yaw rate max, Right: at steady)

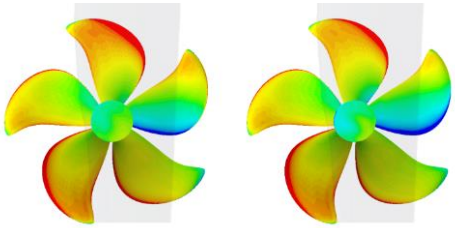

Figure 18 Instantaneous pressure distribution on propeller face side with rudder during STBD turning

(Left: at yaw rate max, Right: at steady)

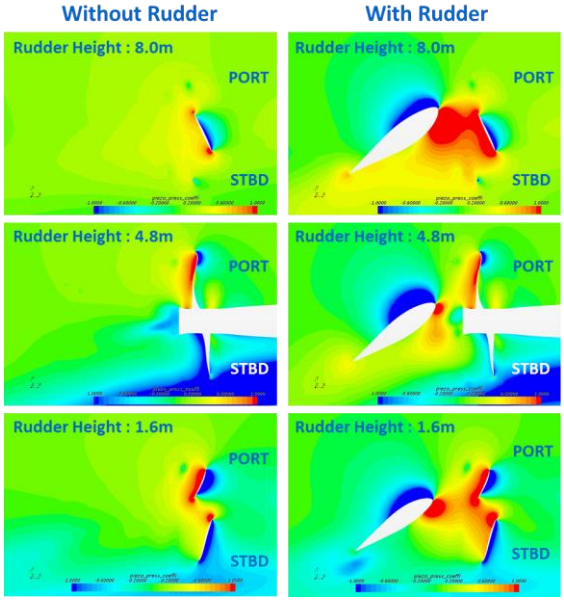

Figure 19 Instantaneous pressure distributions on plane at three different heights during STBD turning

(Left: without rudder, Right: with rudder)

During PORT turning motion, adversely, the direction of flow into propeller is from STBD side to PORT side. Due to the propeller rotation direction, the propeller experiences a count-swirl flow in upper part on the propeller during ship turning motion. Consequently, as shown in Figure 20, it is inferred that the center of thrust even locates in upper part on the propeller without rudder and the vertical moment (Mz) essentially works on reducing the bearing load of stern tube in this condition.

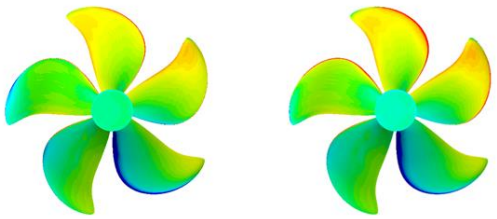

Figure 20 Instantaneous pressure distribution on propeller face side without rudder during PORT turning

(Left: at yaw rate max, Right: at steady)

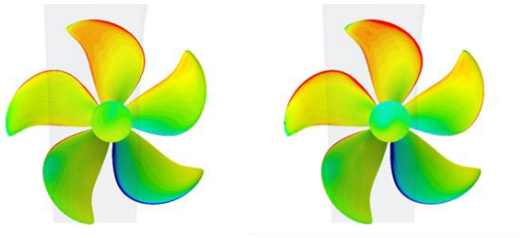

Figure 21 Instantaneous pressure distribution on propeller face side with rudder during PORT turning

(Left: at yaw rate max, Right: at steady)

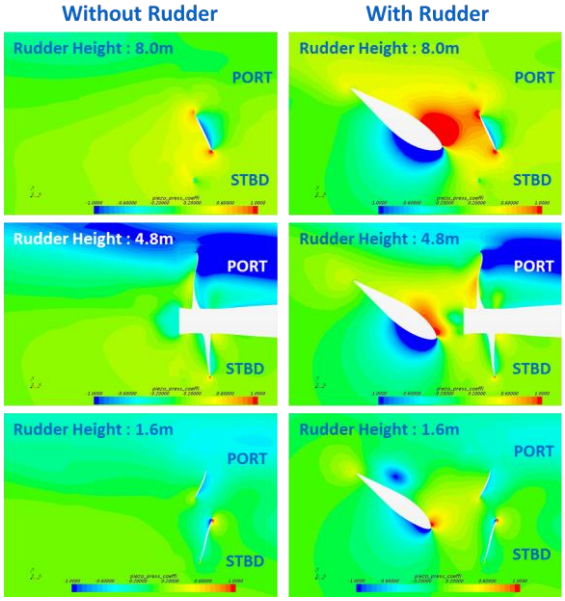

Figure 22 Instantaneous pressure distributions on plane at three different heights during PORT turning

(Left: without rudder, Right: with rudder)

As shown in Figure 21, the pressure on upper part of propeller is also increased by rudder likewise the STBD

turning cases. Although the pressure on lower part of propeller is also increased, the effect by rudder is relatively less than that of STBD turning cases. This can be explained by Figure 22. During PORT turning, the pressure on the lower region of rudder is not significantly increased unlike Figure 19 at same status, yaw rate max.

Moreover, the horizontal moment (My) of propeller was more sensitive to rudder effect rather than vertical moment (Mz) for the ship turning motion. If the rudder is operating for STBD or PORT turning motion of ship, the rudder area facing to the propeller is larger and the rudder is respectively biased to propeller, as shown in Figure 18 and Figure 21. So the pressure distribution on the part of propeller blade facing to biased rudder is mainly changed and the horizontal moment (My) is consequently affected. During the STBD turning, this value was reduced about 20% by the rudder, however, was increased about 2 times during the PORT turning as represented from Figure 13 to Figure 16.

As mentioned in section 2.3, the rudder used in this study was composed by different section along rudder height to prevent the rudder cavitation. This characteristic is also related to asymmetrical effect of rudder on the propeller eccentric forces at each turning direction. By comparing to Figure 24 and Figure 25, it might be explained why the rudder's effect on propeller eccentric forces is asymmetrical as the turning direction of ship. The instantaneous pressure distributions around leading edge of rudder on STBD turning and PORT turning are clearly

different each other, respectively.

Figure 24 Instantaneous pressure distributions on rudder during STBD turning (looking downstream)

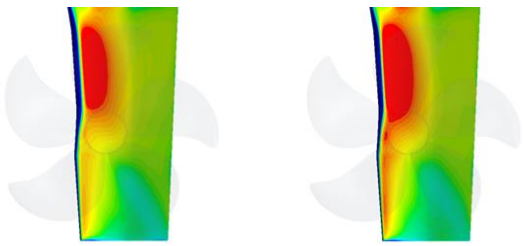

(Left: at yaw rate max, Right: at steady)

Figure 25 Instantaneous pressure distributions on rudder during PORT turning (looking downstream)

(Left: at yaw rate max, Right: at steady)

4 CONCLUSION

In this study, numerical simulations were performed to investigate the effect of rudder existence on propeller lateral forces and moments. The target vessel was chosen as about 10,000TEU class container ship. For straight run, the thrust and torque of propeller were increased by rudder existence, so the propulsive efficiency on propeller was improved by the wake effect of rudder. The effect of rudder on propeller eccentric forces was different according to turning direction. The vertical moment (Mz) directly related to the bearing load of stern tube was about 50% diminished by existence of rudder for STBD turning, while that value was similar each other regardless of rudder existence for PORT turning. This difference is basically oriented by the interaction between propeller's rotation direction and inflow direction to propeller. Especially, the effect of rudder on propeller lateral forces and moments is depends on where the flow straightness behind propeller is relatively strong or weak. Although the center of thrust on propeller is located in lower part of propeller for STBD turning, the magnitude of vertical moment (Mz) is compensated by rudder effect in upper part of propeller. In contrast, the center of thrust on propeller is already located in upper part of propeller for PORT turning so the effect of rudder is relatively limited on propeller eccentric forces. On the other hands, the rudder affects to the horizontal moment (My) of propeller regardless turning direction. And Rudder's main configurations such as leading edge sweep angle, aspect ratio, section shape or distance between propeller and rudder might relate to the propeller eccentric forces. Additionally some appendages located around propeller including rudder and various ESDs have to be considered to estimate reliable propeller eccentric forces.

REFERENCES

American Bureau of Shipping (2018). Guide for Enhanced Shaft Alignment. ABS, USA.

Det Norske Veritas-Germanischer Lloyd (2018). Shaft Alignment, DNVGL-CG-0283. DNV-GL, Norway.

Kuroiwa, R., Oshima, A., Nishioka, T., Tateishi, T., Ohyama, T. & Ishijima, T. (2007). 'Reliability Improvement of Stern Tube Bearing Considering Propeller Shaft Forces during Ship Turning', Mitsubishi Heavy Industries, Ltd., Technical Review Vol. **44**, No. **3**.

Lee, T. G., Song, G. S., Kim, J. N., Lee, J. S. & Park, H. G. (2017). 'Effect of Propeller Eccentric Forces on the Bearing Loads of the Complicated Shafting System for Large Container Ships', Fifth International Symposium on Marine Propulsion SMP'17. Helsinki, Finland.

Shin, S. H. (2015). 'Effects of Propeller Forces on the Propeller Shaft Bearing during Going Straight and Turning of Ship', Journal of the Society of Naval Architects of Korea, Vol. **52**, No. **1**.

Vartdal, B.J., Gjestland, T. & Arvidsen, T.I.(2009). 'Lateral propeller forces and their effects on shaft bearings'. Proceeding on First International Symposium on Marine Propulsors, Trondheim, Norway.